Fuel 409 (2026) 137810

Contents lists available at ScienceDirect

Fuel

journal homepage: www.elsevier.com/locate/fuel

Full Length Article

A comparison of carbon capture and biomass utilisation for decarbonising oxygen blast furnace ironmaking

Cristian Barón, Manuel Bailera, Jorge Perpiñán, Begoña Peña *

Energy and CO_2 Group, Aragon Institute of Engineering Research (I3A), Department of Mechanical Engineering, Escuela de Ingeniería y Arquitectura, Universidad de Zaragoza, María de Luna 3, 50018 Zaragoza, Spain

ARTICLE INFO

Keywords:
Ironmaking
Calcium Looping
Biomass
Oxy-blast furnace
Power-to-gas
Methanation

ABSTRACT

The Iron and Steel industry stands as a significant industrial source of CO_2 emissions, contributing 7% to the global CO_2 emissions. Therefore, innovative methods for CO_2 removal must be developed in the current path to heavy-industry decarbonization. This work presents and compares two low-carbon brownfield concepts, integrated in an existing steelmaking plant, which incorporates power-to-gas technology, top gas recycling and oxygen blast furnace. The first concept captures carbon via calcium looping and uses it as the source for the methanation plant to produce synthetic natural gas, which is injected in the blast furnace as reducing agent. The second concept is based on charcoal and syngas production through biomass pyrolysis. The former is pulverized and injected into the blast furnace, replacing part of the fossil coke used in the reference steelmaking plant. The latter is used as carbon source in the methanation stage, avoiding the carbon capture stage. Promising results are obtained for the concept which uses biomass as carbon source in the process, achieving a CO_2 abatement cost of 64.5 €/t_{CO2}. It is estimated that this cost could be reduced to 55.4 €/t_{CO2} by scale economy. Despite current economic challenges, the potential mid-term profitability, driven by the ongoing deployment of renewable energy, identifies the utilization of biomass as a solution for environmentally conscious steelmaking.

1. Introduction

The Iron and Steel (I&S) industry accounts for 27 % of CO_2 emissions of the overall manufacturing sector [1], and contributes 7 % to the global CO_2 emissions [2]. The targets set by the European Commission in the European Green Deal to achieve carbon neutrality in 2050 require the deployment of decarbonisation techniques for this industry [3]. State-of-the-art of technologies for steelmaking includes three main routes: (1) BF-BOF, blast furnace-basic oxygen furnace, (2) Scrap-EAF, scrap based electric arc furnace, and (3) DRI-EAF, direct reduced iron-electric arc furnace.

The BF-BOF route is the dominant process for steel manufacturing, consisting of a blast furnace that reduces iron ore with coke to produce hot metal. Subsequently, the basic oxygen furnace (BOF) lowers the carbon content of the molten iron to produce the crude steel. It represents 70 % of the global steel production. This route is highly energy and carbon intensive, resulting in 13–14 GJ/t_{HM} net specific energy consumption and 2000–2200 kg_{CO2}/t_{HM} specific carbon emissions [1].

Despite the efforts to achieve a carbon–neutral steel industry by using other less intensive routes (scrap-EAF and DRI-EAF), it is expected that at least 20 % of the current BF-BOF route furnaces, which are responsible for the 14 % of the steelmaking emissions, will still be in operation by 2050 [1]. These furnaces will be only phased-out at relining, which typically takes place every 20–40 years [4]. Therefore, innovative methods for CO_2 removal without substantial changes in the blast furnaces will be highly demanded in the next decades.

Within the I&S industry, amine scrubbing is considered one of the most effective and practical approach for capturing CO_2 emissions from blast furnace gases (BFG) so far [2,5]. However, it has still important challenges, such as the high energy consumption during solvent regeneration, the corrosive properties of the solvent, and its inherent toxicity [2]. CO_2 can also be captured with other technologies, such as Calcium Looping (CaL). Among its advantages, the utilization of limestone as raw material and the high temperature of operation are the most significant. Limestone is extremely cheap and world-wide abundant, as well as non-toxic [6]. Furthermore, the associated high temperatures make it possible to properly reutilize the heat into other lower-temperature processes, thus potentially reducing the energy penalty [7].

CaL has been demonstrated in different pilot plants in Europe [8,9,10] and elsewhere, like USA [11], Canada [12] and Taiwan [13] at TRL 6–7. Regarding CaL in steelmaking, there exist some projects, such

---

* Corresponding author.
E-mail address: bpp@unizar.es (B. Peña).

https://doi.org/10.1016/j.fuel.2025.137810
Received 1 September 2025; Received in revised form 18 November 2025; Accepted 29 November 2025

Nomenclature

Abbreviations

AFT	Adiabatic Flame Temperature
ASU	Air Separation Unit
BF	Blast Furnace
BOF	Basic Oxygen Furnace
BOFG	Basic Oxygen Furnace Gas
BFG	Blast furnace gas
CaL	Calcium Looping
CAPEX	Capital EXPenditure
CFB	Circulating Fluidized Bed
COG	Coke Oven Gas
DRI	Direct Reduced Iron
EAF	Electric Arc Furnace
HM	Hot Metal
I&S	Iron and Steel
KPI	Key Parameter Indicator
LHV	Low Heating Value
Oxy-BF	Oxygen Furnace
OPEX	OPerational EXpenditure
O&M	Operation and Maintenance
PEM	Proton Exchange Membrane
PtG	Power to gas
SEC	Specific electricity consumption
SNG	Synthetic Natural Gas
TGR	Top Gas Recycling
u.h.m.p	Unit of hot metal produced

Latin alphabet

a	model parameter
C_i	CAPEX
e_i	Specific electricity energy consumption
Δe_i	Specific thermal consumption variation with respect to Case 0
E_{CO2}	CO_2 capture efficiency
$E_{penalty}$	Energy penalty
HHV	High heating value
LHV	Low heating value MJ/t
I_i	Incomes
$\dot{m}_{HM}$	Hot metal production
NPV	Net present value (discounted cash flow)
n	Loan amortization period
n_i	Molar flow
M_i	Molar mass of component “i”
O_i	OPEX (biomass)
P	pressure
q_{CaL}	Specific thermal needs of the CaL plant
$r_{i,j}$	Component “i” consumed or produced in “j” per u.h.m.p
r'''	reaction source term
Δr_{CO2}	CO_2 avoided per u.h.m.p
T	temperature

Greek alphabet

α	Economic parameter
β	Economic parameter
γ	Economic parameter
ε	volume fraction
η_{elec}	Energy conversion factor from thermal energy to electricity
ρ	density

as CaLby2030 [14], and a few studies. Tian et al. [7] proposed the integration of CaL and waste recycling technologies into steelmaking, studying the performance of steel slag-derived CO_2 sorbents (mainly composed of lime). Sungsook & Srinophakun [15] simulated a CaL carbon capture plant for a steel plant, analysing its performance for different flue gas stream from the steel plant (100 % coal, 50 % coal + 50 % coke and 100 % coke). Santos and Hanak [5] conducted a review regarding different decarbonisation possibilities for various energy-intensive industries. They found that the mean carbon abatement cost of CaL for steelmaking to be in the range of 32.7 €/t_{CO2}, whereas for amines it is 104.6 €/t_{CO2}. Such a difference is related to the better integration of the calcium looping plant, characterized by the heat waste recovery and the reutilization of lime as feedstock for the steelmaking plant. Carbone et al. [16] modelled two different integrated concepts of CCS-CaL into a steelmaking plant, via the BF-BOF route and the DRI-EAF route. The BF emissions decreased by 74 %, 81 % and 86 % in three different scenarios for the BF-BOF case, compared to the reference case of 2100 kg_{CO2}/t_{steel}. On average, the energy consumption from non-renewables increased by 53 % when CaL was used. In none of these articles was the economic viability of a CaL-based steelmaking plant investigated.

An alternative approach to reduce CO_2 emissions in blast furnaces is the utilization of biomass resources. A commonly adopted method for introducing biomass in ironmaking is the production of biochar, which is the solid product obtained through the torrefaction or pyrolysis of biomass. This process upgrades biomass for ironmaking, achieving similar heating values and O/C and H/C ratios as those found in coal. Nonetheless, the mechanical properties of biochar are worse than coke, so biochar cannot support the burden inside the furnace, only allowing the replacement of around 10 % of the coke introduced at the top (apart from some smaller furnaces in Brazil, where fossil coke is completely substituted [17]). Hence, the industry has chosen the injection of pulverized biochar at the tuyeres to replace the pulverized coal injection. Typical injections rates of biochar are 100–150 kg/t_{HM} [18]. Some authors proposed co-injecting the biochar and the syngas from pyrolysis process in order to increase the biomass utilization [19]. The use of biomass for steelmaking was studied by Bailera et al. [20], even though only the blast furnace was simulated in Aspen Plus. This study combined different decarbonisation techniques for BFs, such as top gas recycling (TGR) and oxy-combustion regime. CO_2 emissions were reduced by 58 %, with energy consumption of 9.8 MJ/kg_{CO2}, and without requiring geological storage. In spite of the promising results, the complete simulation of the plant should be done prior to assess the economic viability.

In summary, the abatement of carbon emissions in the steelmaking industry requires further research on sustainable fuels and carbon capture technologies. In particular, studies on promising alternatives, such as Calcium Looping [5,7,14,16] and biomass [20], are very scarce and incomplete, with no economic assessment published so far.

The novelty of this study is to evaluate for the first time, from both technical and economic perspective, these two potential approaches (carbon capture via CaL and biomass utilization) within the context of a modified steelmaking plant. This modified plant incorporates power-to-gas (PtG) technology and an oxygen blast furnace (oxy-BF).

The detailed process models are implemented in Aspen Plus® for both the reference BF-BOF process plant and the novel proposed concepts. The comparison between the two low-carbon configurations and the reference case involves the analysis of the demand for coal, overall energy consumption, and CO_2 emissions. Sankey diagrams illustrating carbon flows are presented and discussed to quantify the impact of biomass utilization in the steelmaking plant. Finally, the study evaluates the economic feasibility of the proposed integrations, identifying technical and economic conditions necessary to achieve reasonable payback periods.

2. Decarbonisation pathways: Carbon capture vs biomass utilization

The present work compares two low-carbon integrations (carbon capture via CaL vs. biomass utilization via pyrolysis) in an advanced steelmaking plant. This conceptual plant combines top gas recycling, oxygen blast furnace, and PtG technology, as one of the most advanced concepts for decarbonization proposed in literature [21]. They are also compared against a reference steelmaking plant, in which no decarbonization technologies have been included.

Top gas recycling consists on the recycling of part of the blast furnace gas leaving the furnace, back into it. This gas stream has a typical volume composition of 22–24 % CO_2, 20–25 % CO, 0–2 % H_2O, 3–4 % H_2, and 47–53 % N_2 and acts as a reducing agent, diminishing coke consumption. It has to be noted that introducing CO_2 or H_2O to the BF is not desirable, as fuel consumption is increased and the reduction of iron oxides is hindered. A common solution is to include a carbon capture stage before reinjecting the top gas, thus avoiding this negative effect [22,23]. The recycled gas can be injected at tuyeres (lower zone), at the shaft (mid zone), at the preparation zone (upper zone), or at a combination of them as shown in Fig. 1 [2]. Injecting the recirculated gas at the tuyeres allows for a proper interaction between the reducing gas and the solids, but decreases flame temperature. Injections at mid shaft avoid decreasing the flame temperature, but a poor solid–gas interaction is obtained [24]. When injected at the upper zone, the only role of the recirculated gas is to preheat the descending solids. Therefore, the gas is not used as a reducing agent, and the presence of CO_2 is not a problem [24].

The TGR can be combined with the use of oxy-combustion in blast furnaces (oxy-BF, OBF). These furnaces use oxygen as oxidizing agent instead of air, allowing for a higher efficiency and a lower consumption of fuel. However, operation conditions are altered due to the reduction of mass flow related to the absence of nitrogen in the gas composition. The recirculation of a percentage of the BFG stream mitigates this issue increasing the mass flow in the furnace and, thus, the sensible heat of the gas stream.

An attractive alternative for steelmaking decarbonization is the combination of oxy-BF with PtG [25]. PtG technology consumes renewable electricity to produce H_2 via water electrolysis, which reacts with the CO_2 from the ironmaking process to obtain a synthetic natural gas (SNG) [26], avoiding the uncertain geological storage. This SNG is later mainly injected into the BF. Two cases are proposed and analysed in this study to obtain the required CO_2 for the methanation: Case 1 uses carbon capture via CaL (fuelled by COG, and partially by SNG), whereas Case 2 makes use of the CO_2 content in the syngas from biomass pyrolysis, thus avoiding the need of a carbon capture stage. The excess production of steel gases (BFG, BOFG, and COG), once the CaL thermal needs are covered in Case 1, is first utilized to meet the power plant thermal needs. Once these requirements are satisfied, the remaining gases are sold to other industries.

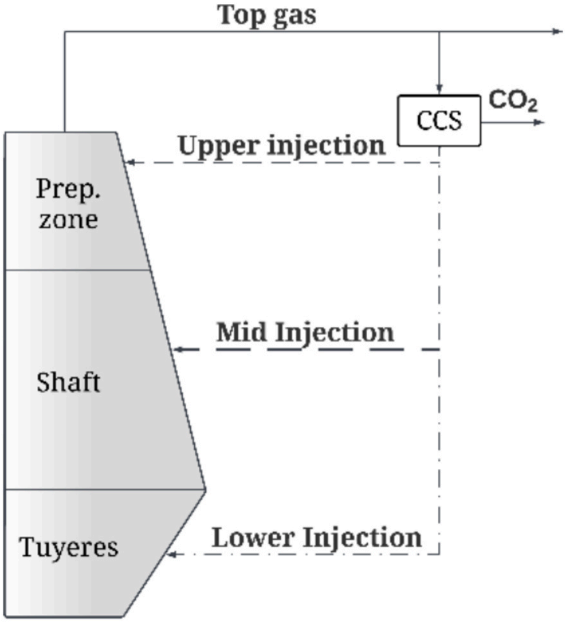

Fig. 1. TGR injection possibilities.

3. Methodology

The models of the reference I&S plant and the two low-carbon concepts are implemented in Aspen Plus v11. The reference case is a conventional BF-BOF plant. Case 0 is described in detail in [27]. The reader is referred there for additional, more comprehensive information about the different modelling blocks of each element of the plant. To summarize, the sinter strand block accounts for the agglomeration process of fine ore particles. In the coke oven model, the coke-making process is simulated, producing coke oven gas (COG) as a by-product. The power plant is run by a percentage of the available COG, BFG, and BOFG and produces 100 MW_e of net electricity for self-consumption [28]. This is a typical figure for integrated steel plants, here considered for comparison purposes. The BOF transforms the hot metal leaving the blast furnace into low/medium-carbon steel, reducing the carbon content from 4.5 wt % C to less than 0.3 wt% C to obtain commercial steel (such as [29]). The blast furnace itself is simulated through a user-defined routine which relates BF inlets and outlets through mass and energy balances, based on the extended operating line methodology [25,26], resulting in the formation of hot metal and BFG. This methodology is based on the Rist diagram, which is generalized to extend its applicability to more scenarios. The most relevant data of the reference BF-BOF plant (Case 0) are presented in Table 1.

Both low-carbon concepts share some technical assumptions: (i) TGR; (ii) an enriched hot blast with O_2 to reach 95 vol% O_2 at the inlet, obtaining an oxy-blast furnace; (iii) production of O_2 and H_2 in an electrolyzer; (iv) a methanation plant.

The selected electrolyzer is taken from the Nel Hydrogen catalogue, with an assumed energy consumption of 3.75 kWh/Nm^3_{H2} [30]. PEM is selected as the electrolysis technology, as it presents a better dynamic response compared to an alkaline electrolyser, as well as other advantages such as a higher energy density and a more compact design. Even though SOEC is rapidly emerging at a commercial scale, its specific costs are still higher, due to cost-learning curve effects. The methanation plant consists of two isothermal fixed-bed reactors operating at 300–350 °C and 5 bar, as by the technology proposed by Hitachi Zosen [31].

Case 1 and Case 2 are presented in Section 3.1 and Section 3.2, respectively. For comparison purposes, the analysis is carried out using specific units per ton of hot metal produced in the BF (t_{HM}), and then scaled up to net amounts for a specific steelmaking plant with a production of 320 t_{HM}/h [32]. The3 economic parameters and the key parameter indicators (KPIs) are described in Section 3.3 and Section 3.4, respectively.

Table 1
Relevant data of Case 0.

Description	Value	Units
CO_2 emissions	1943	kg/t_{HM}
Coal consumption	668	kg/t_{HM}
Sold steel gases	2400	MJ/t_{HM}

3.1. Case 1: CaL integration

The Calcium Looping system captures the CO_2 from the BFG to be combined with electrolytic H_2. The resultant SNG is injected into the blast furnace (Fig. 2). The amount of SNG produced is the required to cover the blast furnace needs, while the calciner is directly fuelled by the surplus COG (therefore, it is not redirected to the power plant). As COG alone is not sufficient to cover the thermal needs of the CaL plant, some extra SNG is produced to cover for the remaining heat. The required SNG establishes the size of the methanation plant, the electrolyzer and the CaL system. The excess heat from the carbonator and the methanation reactors is used to feed the power plant, reducing the process gases consumption.

The model implemented in Aspen Plus of the CaL system is illustrated in Fig. 3. The make-up flow is introduced through the carbonator in order to preheat it, so less thermal energy is needed in the calciner [9]. Two heat-exchangers have also been included. One utilizes the heat of the CO_2 leaving the calciner to preheat the fuel mixture ((COG + SNG) + O_2), while the other utilizes the heat of the clean BFG to preheat the BFG to be cleaned [8]. The calciner has been modelled as a mixed chamber CFB (Circulating Fluidized Bed) under oxy-combustion conditions, in which O_2 and COG enter from the bottom, fluidizing the particles. CO_2 is recirculated to approximate to the air-combustion conditions (O_2:CO_2 ratio of 21:79) at the inlet [33]. The carbonator, also modelled as a CFB, has been divided into various sections to properly reproduce the carbonation rate along the reactor [34]. The water present in the captured CO_2 stream is condensed before leaving the system.

The input data are summarized in Table 2. The residence time of the carbonator is left as a dependant variable to obtain a 90 % CO_2 capture efficiency (E_{CO2}) [35] at reactor outlet. Meanwhile, the calciner residence time is fixed to 5 s, which is a common, conservative value for calcination CFB reactor [8,36], enough for a 100 % conversion. The ratios F_R/F_{CO2} (molar ratio between solids recirculated and CO_2 in the flue gas make-up) and F_0/F_R (molar ratio between make-up and solids recirculated CO_2) are associated to the molar flows indicated in Fig. 3. 10 % heat losses are also assumed for both reactors [37].

These ratios are adjusted from the work of Abanades [38], in which those ratios are related to obtain 90 % capture efficiency. As in that work the make-up is introduced in the calciner, not the carbonator, it is necessary to modify the ratios. The mathematical calculation is detailed in the Supplementary Document.

The Aspen models for calciner and carbonator are presented in Fig. 4. As mentioned before, the calciner is built as a mixed chamber CFB. The COG + SNG is combusted at the bottom of the reactor, mixing with the recirculated CO_2 and the solids stream. The calciner reactor is modelled as a single continuously stirred tank reactor, since calcination is an almost instant reaction. Finally, a valve takes account of the pressure drop occurring within the reactor. COG + SNG combustion is considered stoichiometric and complete. The heat released in combustion covers the endothermic processes of (i) heating of the solids at the inlet and (ii) calcination reaction.

Regarding the carbonator, the BFG and the solids enter through the bottom, mixing before entering the carbonator. It is assumed that the hot solid stream partially preheats the BFG stream.

The carbonation reactor is simulated connecting seven continuous stirred tank reactors (CSTR) in series to compute the carbonation of the sorbent along the reactor [43,44]. This configuration leads to a variation below 1 % in the CO_2 capture efficiency for residence times from 3 to 12 s, expected for a CFB reactor [45]. The inlet pressure of each reactor is decreased to simulate the real pressure drop. Finally, the kinetics of carbonation and calcination is implemented according to Eqs. (1)-(2). These equations were modelled for operation inside a coal-based CFB boiler, in which gasification reactions occur. Therefore, they are suitable for high H_2 and CO conditions, such as the ones presented in the CO_2 capture of BFG [46].

$$r_{calc}^{triple\ prime} = 1.22{*}exp\left(\frac{-4026}{T}\right)\left(P_{eq} - P_{CO2}\right)\left(A_{m0,CaCO3}\right)\varepsilon_{CaCO3}\,\rho_{CaCO3} \tag{1}$$

$$r_{carb}^{triple\ prime} = 0.0169, exp\left(\frac{-3488}{T}\right)\left(P_{CO2} - P_{eq}\right)A_{m0,CaO}\,\varepsilon_{CaO}\,\rho_{CaO} \tag{2}$$

where T represents the temperature (K), P_{eq} the equilibrium pressure (atm) of the calcination reaction at the given temperature, P_{CO2} the CO_2 partial pressure (atm), A_{m0} the specific surface areas (300 m^2/kg for $CaCO_3$ and 20000 m^2/kg for CaO), ρ the density (kg/m^3) and ε the volume fraction (p.u).

3.2. Case 2: Biomass integration

Case 2 (Fig. 5) includes the pyrolysis of biomass, obtaining charcoal, syngas and bio-oil [20]. As opposed to Case 1, no carbon capture stage is

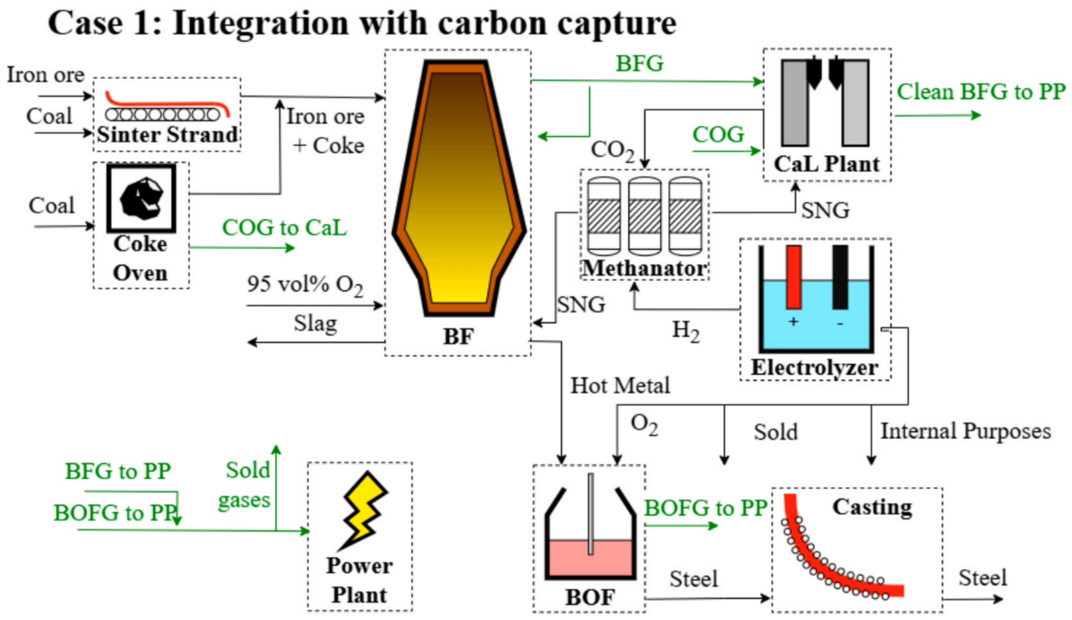

Fig. 2. Process flow diagram for the carbon capture integration.

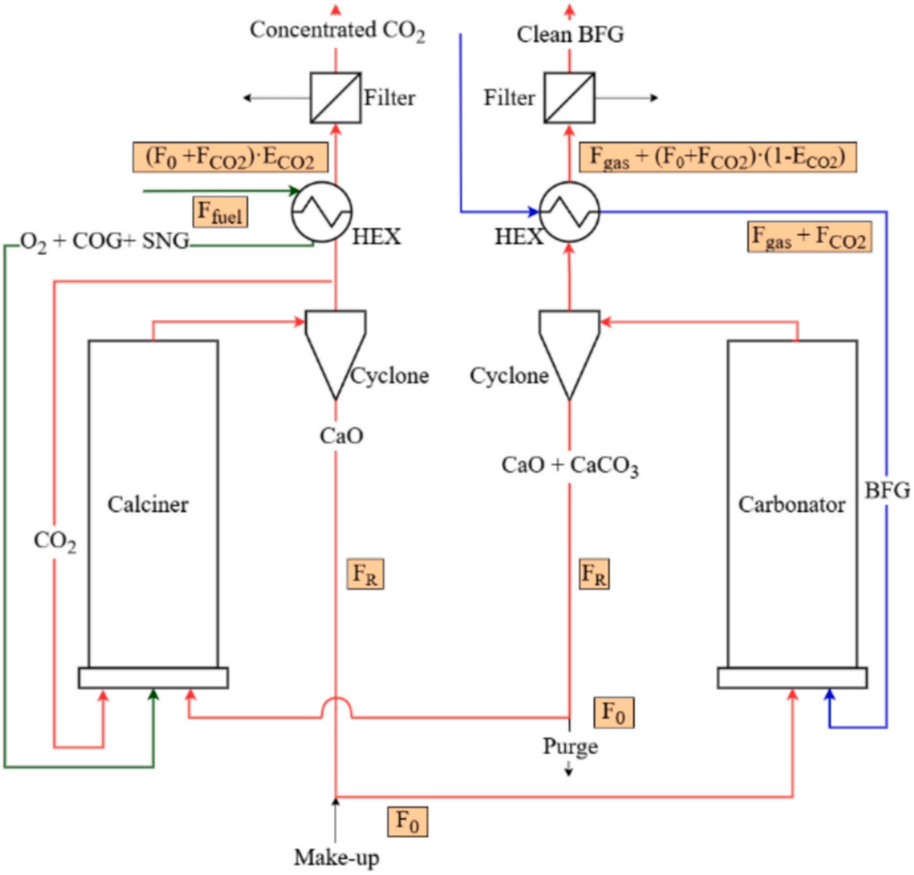

Fig. 3. Aspen Plus model of the CaL system.

Table 2
Input data of the CaL system.

Variable	Value	Units	Ref.
CO_2 capture efficiency	0.9	–	
Cyclone efficiencies	0.999	–	[33]
Condenser temperature	25	°C	
O_2 at calciner inlet	21	vol%	[33]
F_r/F_{CO2}	6	–	[38]
F_0/F_R	0.03	–	[38]
Calciner			
Temperature	900	°C, uniform	[39,40]
Pressure loss	0.15	bar	[41]
Heat losses	10	%	[37]
Residence time	5	s	[8,36]
Carbonator			
Temperature	650	°C, uniform	[39,40]
Pressure loss	0.15	bar	[42]
Heat losses	10	%	[37]

required, as CO_2 supplies for the methanator are provided by the syngas. Furthermore, the syngas benefits from a high H_2 content, as well as the presence of CH_4, both leading to a decrease of the electrolyzer size and electricity consumption.

The real data obtained from the experiments on slow pyrolysis of Solar et al. [47] are considered to model the pyrolysis stage. Specifically, the slow pyrolysis of Pinus Radiata is performed at 700 °C for 30 min, yielding 24.3 % of solid phase, 50.8 % of gas phase, and 24.9 % of liquid phase. Proximate and immediate analyses of the solid phase before and after treatment are compiled in Table 3. The composition of the gas obtained (from now on, syngas) is detailed in Table 4. The liquid phase is not utilized in the present work. However, it could be processed into biofuels, or transformed via petrochemical routes into valuable chemicals that could be used in fields such as pharmacology, food or polymer chemistry [48].

The biomass treatment plant (pyrolysis and grinding) is not modelled in detail in Aspen Plus. The associated energy and cost of the plant are computed externally after determining the biomass production requirements of the plant and sizing it. The plant is sized by the charcoal needs of the blast furnace, which fixes the amount of biomass to be pyrolyzed, and also the syngas production. The CO_2 emissions associated for this process are considered 0.0155 kg_{CO2}/MJ [49]. Its energy consumption is typically estimated in literature as being within the 6–15 % of the biomass high heating value (HHV) [50]. The least optimistic value (15 %) is considered, so that the obtained energy penalty corresponds to the worst potential scenario.

The blast furnace integration is based on the work of Bailera et al. [20]. The top gas recycled is injected through the upper part. It is oxy-combusted before entering the furnace back to increase the temperature, so an almost-pure CO_2 stream is obtained. As it was mentioned, the gas is not used as a reducing agent when injected at the preparation zone, so the presence of CO_2 is not a problem.

3.3. Economic parameters

For the economic analysis, a time horizon of 20 years with an annual interest of 4 % is considered. Table 5 summarizes the correlations and parameters used. The initial capital expenditure (CAPEX) accounts for the investment costs related to methanation, electrolyser and retrofitting the blast furnace for oxy-combustion operation, as well as other direct and indirect costs such as the installation or the engineering costs. The cost of the CaL plant is also considered in Case 1 and the cost of the pyrolysis plant in Case 2. The operational expenditure (OPEX) includes the catalyst renovation (15 % yearly), the water consumption (1.47 €/t),

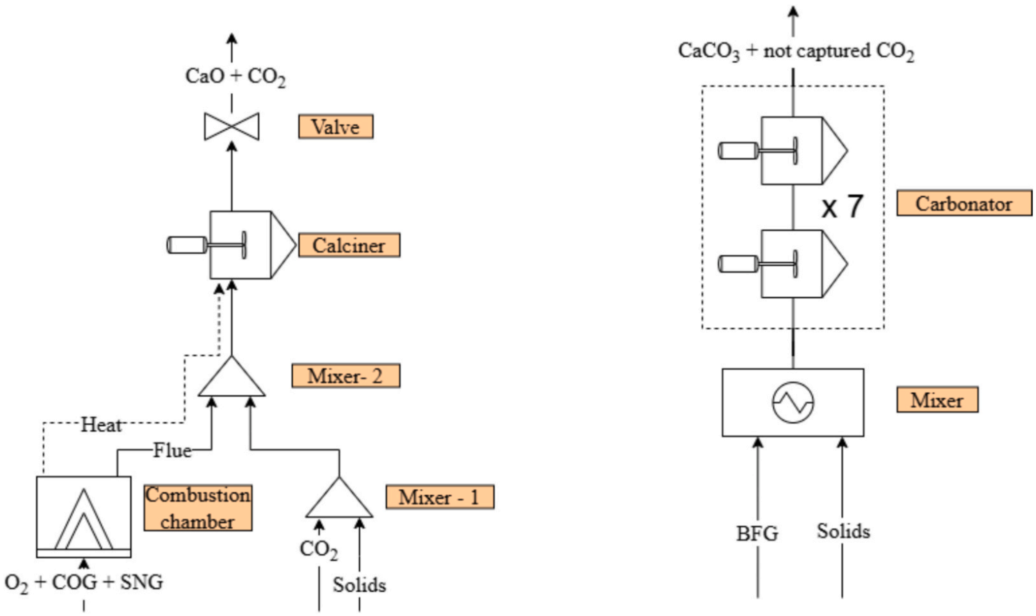

Fig. 4. Left: Aspen Plus calciner model; Right: Aspen Plus carbonator model.

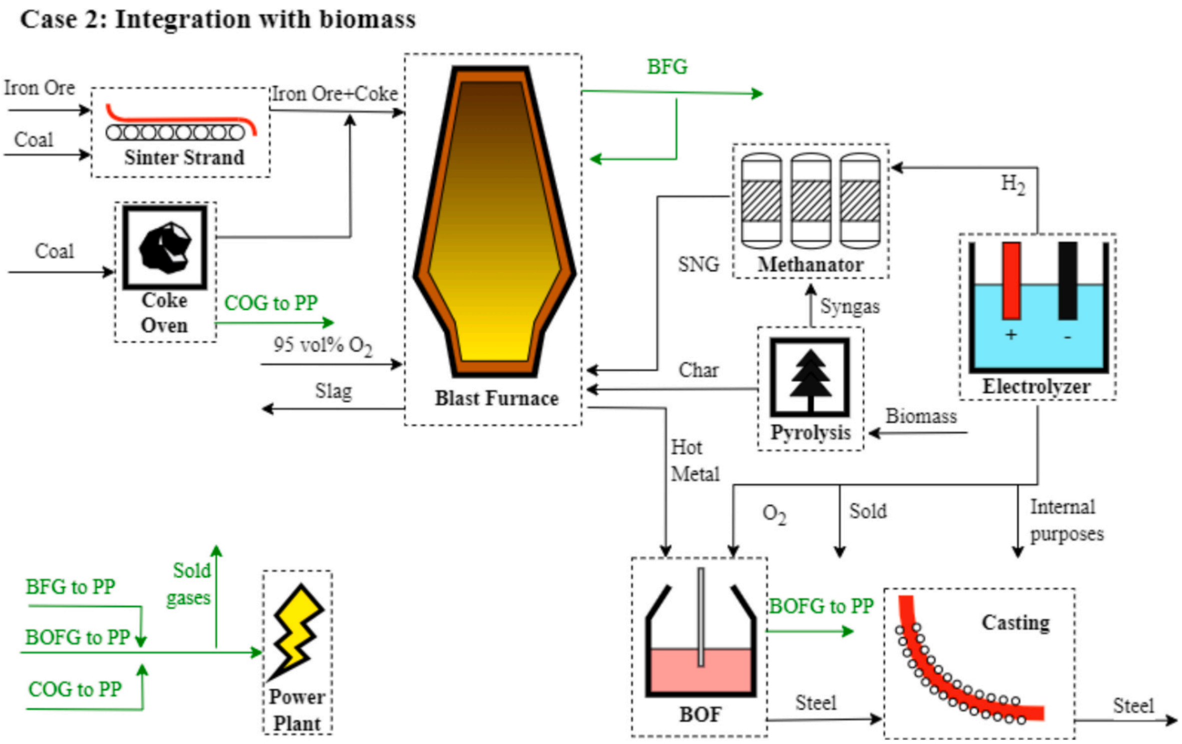

Fig. 5. Process flow diagram for the biomass integration.

the electricity purchased (60.3 €/MWh), the operation and maintenance (3 % of total CAPEX), as well as the limestone renovation (Case 1) or the biomass demand (Case 2). The biomass cost includes the associated costs of all the logistic process, including transportation, grinding and pyrolysis. Annual incomes summarize the excess O_2 by-produced in the electrolyzer, sold at 80 €/t, the flared excess steel gases, whose energy is sold at 19.6 €/MWh, the CO_2 tax avoided (84 €/t_{CO2}) and the coal saved thanks to the integration, bought at 149.3 €/t. Although steelmaking industry operates under continuous production, service and maintenance stops are also considered, rendering an equivalent of 8000 h of production per year.

3.4. Key performance indicators

A total of 18 KPIs are calculated to evaluate and compare the obtained results. KPIs 1 to 12 correspond to the system operation. KPI 1 is the specific primary energy consumption per unit of hot metal produced (MJ/t_{HM}) required in the form of thermal energy for the system responsible of abating the CO_2 emissions in each case. This approach is straightforward for Case 1, as it integrates a carbon capture plant whose thermal energy consumption is calculated in the Aspen Plus simulation. For Case 2, the reduction in CO_2 emissions is accomplished here by the use of carbon–neutral biomass. Therefore, KPI 1 is calculated

Table 3
Characterization of the solid biomass re[,]

	Biomass	Charcoal
Proximate analysis (wt%)		
Moisture	10.6	2.1
Volatile matter	70.7	10.6
Ash	0.6	4.2
Fixed carbon	18.1	83.1
Elemental analysis (wt% daf)		
C	47.8	99.0
H	7.6	0.4
O	44.6	0.5
N	0.0	0.1
HHV (MJ/kg)	16.4	32.8

Source 2047.

Table 4
Characterization of the syngas obtained from slow pyrolysis [20,47].

Compound	vol%
H_2	39.0
CO	29.2
CO_2	16.3
CH_4	14.5
C_2H_4	0.7
C_2H_6	0.3
HHV (MJ/kg)	18.0
HHV (MJ/Nm^3)	13.8

Table 5
Main assumptions for economic analysis.

	Cost equation (M€) or (M€/y)	Parameters α, β, γ	Ref.
CAPEX			
BF Oxy-Retroffiting	$0.5 \bullet \alpha$	BF renovation cost [M€]	[1]
Pyrolysis plant			
Rotary kiln	$1.88 \bullet (\alpha/1400)^{0.65}$	Biomass consumption [kg/h]	[51]
Biomass dryer	$2.015 \bullet (\alpha/1400)^{0.65}$	Biomass consumption [kg/h]	[51]
Calcium Looping			
Calciner	$0.193 \bullet \alpha^{0.65}$	Thermal power [MWt]	[52]
Carbonator	$0.217 \bullet \alpha + 3.83$	Low heating value [MWt]	[52]
Heat exchangers	$(9016.3 + 721.3 \bullet \alpha^{0.8}) \bullet 10^{-6}$	Area [m^2]	[53]
Electrolyser	$400 \bullet 10^{-6} \bullet \alpha$	Power [kW]	[54]
Methanation			
Compressors	$0.267 \bullet (\alpha/445)^{0.67}$	Power [kW]	[55]
Reactors	$300 \cdot 10^{-6} \bullet \alpha$	SNG power [kW$_{SNG}$]	[56]
Catalyst	$0.1875 \bullet \alpha$	Volume of catalyst [m^3]	[55]
Other direct costs			
Installation	$39\ \% \bullet \alpha$	Total equipment costs [€]	[57]
Instrumentation & control	$26\ \% \bullet \alpha$	Total equipment costs [€]	[57]
Piping	$31\ \% \bullet \alpha$	Total equipment costs [€]	[57]
Electrical	$10\ \% \bullet \alpha$	Total equipment costs [€]	[57]
Building	$29\ \% \bullet \alpha$	Total equipment costs [€]	[57]
Indirect costs			
Engineering	$32\ \% \bullet \alpha$	Total equipment costs [€]	[57]
Legal expenses	$4\ \% \bullet \alpha$	Total equipment costs [€]	[57]
Construction expenses	$34\ \% \bullet \alpha$	Total equipment costs [€]	[57]
Contingency	$37\ \% \bullet \alpha$	Total equipment costs [€]	[57]
OPEX			
Biomass & treatment	$2.82 \bullet 10^{-3} \bullet \alpha$	Charcoal consumption [kg/h]	[58]
Limestone renovation	$10^{-5} \bullet \alpha$	Limestone renovation [t/y]	[59]
Catalyst renovation	$15\ \% \bullet \alpha$	Initial catalyst cost [M€]	[60]
Electricity	$6.03 \bullet 10^{-5} \bullet \alpha$	Electricity consumption [MWh/y]	[61]
Water	$1.47 \bullet 10^{-6} \bullet \alpha$	Water consumption [m^3/y]	[62]
O&M	$3\ \% \bullet \alpha$	Total CAPEX	[57]
INCOMES			
Oxygen	$80 \bullet 10^{-6} \bullet \alpha$	O_2 generated [t_{O2}/y]	[63]
Flared gases	$(15 + \alpha^{*}\beta/13) \bullet \gamma \bullet 10^{-6}$	α = NG Price [€/MWh]; β = Steel gases LHV [kWh/kg]; γ = Steel gases generated [MWh/y]	–
Coal avoided	$1.49 \bullet 10^{-4} \bullet \alpha$	Coal avoided [t_{coal}/y]	[64]
CO_2 taxes	$84 \bullet 10^{-6}\ {}^{*}\alpha$	CO_2 consumed [t_{CO2}/y]	[65]

considering the thermal energy consumption in the biomass treatment unit, according to Eq. (3).

$$KPI\,1_{C,2} = r_B(15\%\,HHV_B) \tag{3}$$

Where r_B is the ratio of biomass consumed (kg/t_{HM}), and HHV_B is its high heating value (MJ/kg). The criterion for the sizing of both systems, CaL plant and pyrolysis plant, is that the adiabatic flame temperature (AFT) in the blast furnace should not drop below 2000 °C for technical reasons [66]. This technical limit defines how much auxiliary fuel can be injected through the tuyeres, thus defining the amount of SNG and biomass to be introduced, which is directly related to the CO_2 needs of the methanization plant. Sizes of methanation and electrolyzer are then established accordingly.

KPI 2 represents the amount of SNG produced in the methanation system, KPI 3 the coke consumption of the blast furnace, and KPI 4 the total coal consumption of the plant, taking into account other processes such as the sintering or cokemaking stages. KPI 5 is exclusive of Case 2, and refers to the charcoal injected into the blast furnace. KPIs 6 and 7 are the equivalent gross and net CO_2 emissions to the atmosphere of the whole steelmaking plant, respectively. The gross emissions are the summation of the flue emissions of all the different elements of the plant. These are the sinter, coke oven, BF stoves, BOF, casting, electricity generation in the power plant, and also the excess steel gases, which will be eventually burnt by other industries, releasing CO_2 which is also accounted here. For Case 1, gross and net CO_2 emissions are equal. For Case 2, they differ, as part of the carbon input of the system comes from biomass, which is considered CO_2-neutral in nature. Therefore, its associated emissions are deducted. This is achieved following Eq. (4).

$$KPI_7 = KPI_6 - \left(\sum_{i=CO_2,CO,CH_4} n_{i,syn} + \sum_{i=C_2H_4,C_2H_6} 2\ n_{i,SYN} + n_{CC,C} \right) M_{CO2} \tag{4}$$

Where $n_{i,syn}$ is the molar flow of the different compounds present in the syngas (kmol/t_{HM}), $n_{cc,c}$ the molar flow of charcoal (kmol/t_{HM}), and M_{CO2} the molar mass of CO_2 (kg/kmol). Essentially, this equation subtracts all the carbon content introduced through the biomass input, either in the form of charcoal, or in the form of the different organic compounds present in the syngas.

The steel gases not used in the power plant are sold. The economic valorization is estimated through the energy content of the gas sold, which is included in KPI 8 by considering the corresponding LHV. The electrolyzer energy consumption is provided in KPI 9. KPI 10 computes the whole electricity consumption. KPI 11 refers to the oxygen needs. In the case that the electrolyzer covers the O_2 needs of the whole plant, a net O_2 excess may be obtained. Otherwise, the air separation unit (ASU) covers the O_2 default. Depending on whether KPI 11 is positive or negative, this quantity represents the surplus O_2 or the amount produced by the ASU, respectively. The energy penalty (KPI 12) is defined as the specific net electrical energy consumed in the industry per kg of CO_2 avoided for each case scenario (Eq. (5)).

$$E_{penalty} = \left(\Delta e_{cons} - \Delta e_{coal} \cdot \eta_{elec} - \Delta e_{gases} \cdot \eta_{elec} + \Delta e_{biomass} \cdot \eta_{elec} \right) / \Delta r_{CO2} \left[MJ/kg_{CO2} \right] \tag{5}$$

Where Δe_{cons} is the specific additional electricity consumed in the industry with regard the reference case (MJ/t_{HM}), Δe_{coal} is the specific coal energy avoided (MJ/t_{HM}), Δe_{gases} is the specific excess of gases sold to nearby industries (KPI 8), $\Delta e_{biomass}$ is the specific primary energy consumption of the pyrolysis (KPI $1_{C,2}$), which is 0 in Case 1. The energy needs of the CaL are supplied by COG, which is not necessary to include here, and part by SNG, which is included in the additional electricity term. η_{elec} is the energy conversion factor from thermal energy to electricity (0.33) and Δr_{CO2} is the amount of CO_2 avoided (kg_{CO2}/t_{HM}).

The results from the economic analysis are summarized in the values of KPIs 13 to 18. KPIs 13 and 14 are the CAPEX and the yearly annual benefits, respectively. KPI14 is the difference between KPI 15 (incomes) and KPI 16 (OPEX). KPIs 17 (CO_2 avoidance cost) and 18 (specific implementation cost) are calculated by Eqs. (6) and (7).

$$KPI17\,[€/t_{CO2}] = 10^{6}\frac{\left(\frac{KPI13}{n} - KPI14\right)}{\dot{m}_{HM}{}^{*}\Delta r_{CO2}} \tag{6}$$

$$KPI18\,[€/t_{HM}] = 10^{6}\frac{\left(\frac{KPI13}{n} - KPI14\right)}{\dot{m}_{\mathrm{HM}}} \tag{7}$$

Where n represents the loan amortization period (in this case, 20 years), Δr_{CO2} the amount of CO_2 avoided yearly (t_{CO2}/y) and $\dot{m}_{HM}$ the annual hot metal production (t_{HM}/y). The 18 KPIs are summarized in Table 6. Accordingly, the parameters utilized alongside this section are summarized in Table 7.

Table 6
KPI description.

KPI	Description	Unit	Calculated as
1	Specific primary energy consumption (SPEC)	MJ/t_{HM}	C1: q_{CaL} C2: $r_B \bullet (15\ \%\ HHV_B)$
2	SNG production	kg_{SNG}/t_{HM}	C1: $r_{SNG,BF} + r_{SNG,CaL}$ C2: $r_{SNG,BF}$
3	Coke consumption	kg_{coke}/t_{HM}	$r_{coke,BF} + r_{coke,sinter}$
4	Total coal consumption	kg_{coal}/t_{HM}	$r_{coal,BF} + r_{coke,sinter} + r_{coal,coke}$
5	Charcoal injected into BF.	kg/t_{HM}	C1: Not applicable C2: Rist Diagram [25,26]
6	Gross CO_2 emissions	kg_{CO2}/t_{HM}	$r_{CO2,BF} + r_{CO2,sinter} + r_{CO2,coke} + r_{CO2,PP} + r_{CO2,sold} + r_{CO2,cast}$
7	Net CO_2 emissions	kg_{CO2}/t_{HM}	C1: KPI 6C2: KPI 6 – $(n_{CO2,syn} + n_{CO,syn} + n_{CH4,syn} + 2 \bullet (n_{C2H4,syn} + n_{C2H6,syn} + n_{CC,C})) \bullet M_{CO2}$
8	Energy content of sold gases	MJ/t_{HM}	$r_{sold} \bullet LHV_{sold}$
9	Electrolyzer energy consumption	MWh/t_{HM}	$e_{PEM} \bullet r_{H2}$
10	Net electricity consumption	MWh/t_{HM}	C1: $e_{PEM} + e_{equipment}$ C2: $e_{PEM} + e_{ASU} + e_{equipment}$
11	Net oxygen balance	kg_{O2}/t_{HM}	C1: $r_{O2,PEM} - r_{O2,BF} - r_{O2,CaL}$ C2: $r_{O2,PEM} - r_{O2,BF} - r_{O2,BFG}$
12	Energy penalty of low-carbon concepts	MJ/kg_{CO2}	$(\Delta e_{cons} - \Delta e_{coal} \bullet \eta_{elec} - \Delta e_{gases} \bullet \eta_{elec} + \Delta e_{biomass} \bullet \eta_{elec}) / \Delta r_{CO2}$
13	CAPEX	$M€$	C1:$C_{PEM} + C_{met} + C_{CaL} + C_{direct} + C_{indirect}$ C2: $C_{PEM} + C_{met} + C_{bio} + C_{direct} + C_{indirect}$
14	Yearly benefits	$M€/y$	KPI 15 – KPI 16
15	Yearly incomes	$M€/y$	C1:$I_{CO2} + I_{O2} + I_{coal} + I_{sold}$ C2:$I_{CO2} + I_{coal} + I_{sold}$
16	OPEX	$M€/y$	C1: $O_{Elec} + O_{O\&M} + O_{cat} + O_{water} + O_{CaCO3}$ C2: $O_{Elec} + O_{O\&M} + O_{cat} + O_{water} + O_{bio}$
17	CO_2 avoidance cost	$€/t_{CO2}$	$10^6 \bullet \frac{NPV_{,20years}}{\dot{m}_{HM} \bullet n \bullet \Delta r_{CO2}}$
18	Specific implementation cost	$€/t_{HM}$	$10^6 \bullet \frac{NPV_{,20years}}{\dot{m}_{HM} \bullet n}$

Table 7
Parameters utilized to calculate KPIs. Specific variables, indicated in small letters, are referred to unit of hot metal produced (u.h.m.p).

Parameter	Description	Units
C_{bio}	CAPEX (biomass treatment plant)	$M€$
C_{CaL}	CAPEX (calcium looping plant)	$M€$
C_{direct}	CAPEX (other direct costs)	$M€$
C_{met}	CAPEX (methanator)	$M€$
$C_{indirect}$	CAPEX (indirect costs)	$M€$
C_{Elec}	CAPEX (electrolyzer)	$M€$
e_{ASU}	Specific electricity consumption (SEC) by ASU	MWh/t_{HM}
$e_{equipment}$	SEC by auxiliary equipment	MWh/t_{HM}
e_{PEM}	SEC by electrolyzer	MWh/t_{HM}
Δe_{coal}	Specific coal energy avoided	MJ/t_{HM}
Δe_{cons}	SEC	MJ/t_{HM}
Δe_{gases}	Specific excess steel gases energy	MJ/t_{HM}
$\Delta e_{thermal}$	Specific primary energy consumed	MJ/t_{HM}
HHV_b	High heating value of biomass	MJ/t
I_{coal}	Incomes (coal cost saving)	$M€/y$
I_{CO2}	Incomes (CO_2 tax saving)	$M€/y$
I_{O2}	Incomes from O_2 sold	$M€/y$
I_{sold}	Incomes from sold gases	$M€/y$
LHV_{sold}	Low heating value of sold gases	MJ/t_{HM}
M_{CO2}	Molar mass of CO_2	kg/mol
$\dot{m}_{HM}$	Hot metal production	t_{HM}/y
NPV	Net Present Value (discounted cash flow)	$M€$
n	Loan amortization period	y
$n_{CC,C}$	Molar flow of charcoal per u.h.m.p	$kmol/t_{HM}$
$n_{i,syn}$	Molar flow of component “i” in syngas per u.h.m.p	$kmol/t_{HM}$
O_{bio}	OPEX (biomass)	$M€/y$
O_{CaCO3}	OPEX (limestone)	$M€/y$
O_{cat}	OPEX (catalyst)	$M€/y$
O_{Elec}	OPEX (electricity)	$M€/y$
$O_{O\&M}$	OPEX (operation and maintenance)	$M€/y$
O_{water}	OPEX (water)	$M€/y$
r_B	Biomass consumed in BF per u.h.m.p	kg/t_{HM}
$r_{i,j}$	Component “i” consumed in “j” per u.h.m.p	kg_i/t_{HM}
$r_{CO2,j}$	CO_2 emitted in “j” per u.h.m.p	kg_{CO2}/t_{HM}
r_{H2}	H_2 produced by electrolyzer per u.h.m.p	kg_{H2}/t_{HM}
r_{sold}	Sold gases per u.h.m.p	kg/t_{HM}
Δr_{CO2}	CO_2 avoided per u.h.m.p	kg_{CO2}/t_{HM}
q_{CaL}	Specific thermal needs of the CaL plant	MJ/t_{HM}
η_{elec}	Energy conversion factor from thermal energy to electricity	–

4. Results and discussion

4.1. Technical assessment

KPIs vary notably between the two analysed concepts as presented in Table 8. The results will also be compared with a study from Perpiñán et al. [21], which proposed a low-carbon integration homologous to the CaL one, using amine scrubbing instead. Regarding KPI 1, the thermal energy required per mass of hot metal produced for the pyrolysis of biomass is lower than the thermal energy required to operate the calciner in the CaL plant. Nonetheless, it has to be stated that, due to the high-temperatures of the CaL process, most of this energy is reutilized in the power plant. The amount of SNG (KPI 2) to be produced is also lower in the biomass case (212.5 kg/t_{HM} vs. 144.4 kg/t_{HM}). The reasons are twofold. Firstly, the injection of biochar in the BF as auxiliary fuel reduces the SNG demand into the BF, which is 195 kg_{SNG}/t_{HM} for Case 1. Secondly, some additional SNG has to be produced in Case 1 to complement the COG in the calciner. The amine-based studied by Perpiñán et al. [21] required also 195 kg_{SNG}/t_{HM} for the BF, but no extra SNG had to be produced for other purposes.

KPIs 3 to 5 are calculated in Aspen Plus®, according to the extended operating line methodology [26]. The utilization of alternative reducing agents, such as SNG or biochar, makes it possible to reduce the coke

Table 8
Comparison of KPIs. Best case for each KPI is highlighted in bold. Last column reflects the percentual change of Case 2 with respect to Case 1.

KPI	Related to	Description	Units	Case 1	Case 2	%
1	Operation	Thermal energy required	MJ/t_{HM}	1592	**1308**	**−18**
2	Operation	SNG produced	kg_{SNG}/t_{HM}	212.5	**144.4**	**–32**
3	Operation	Coke rate	kg_{coke}/t_{HM}	278.5	**223.3**	**−20**
4	Operation	Total coal consumption	kg_{coal}/t_{HM}	446.6	**373.0**	**−16**
5	Operation	Charcoal injected	kg/t_{HM}	–	129.3	–
6	Operation	Gross CO_2 emissions	kg_{CO2}/t_{HM}	**1272**	1971	+55
7	Operation	Net CO_2 emissions	kg_{CO2}/t_{HM}	1272	**1138**	**−10**
8	Operation	Sold steel gases	MJ/t_{HM}	4684	**5322**	**+14**
9	Operation	Electrolyzer size	MWh/t_{HM}	4.32	**1.421**	**−67**
10	Operation	Net electricity consumption	MWh/t_{HM}	4.46	**1.60**	**−64**
11	Operation	O_2 balance	kg_{O2}/t_{HM}	**14.95**	–333	–
12	Operation	Energy penalty	MJ/kg_{CO2}	19.29	**6.18**	**−68**
13	Economics	CAPEX	*M€*	2721	**1515**	**−44**
14	Economics	Benefits	*M€/y*	−510.9	**−84.12**	–
15	Economics	Incomes	*M€/y*	263.8	**326.7**	**+24**
16	Economics	OPEX	*M€/y*	774.7	**410.8**	**−47**
17	Economics	CO_2 avoidance cost	*€/*t_{CO2}	281.4	**64.5**	**−77**
18	Economics	Specific implementation cost	*€/*t_{HM}	188.8	**51.9**	**−73**

consumption to 278.5 (same as [21]) and 223.2 kg/t_{HM} for case 1 and 2, respectively (KPI 3). Pulverized coal is fully substituted in both proposed concepts, so coal consumption comes entirely from two sources: (i) the small quantity used for sintering and (ii) the raw material for coke production. Therefore, coal consumption is directly related to coke consumption, allowing for a lesser coal consumption in case 2 (KPI 4). Reductions of 33 % and 44 % with respect to case 0 (668 kg/t_{HM}) are obtained, respectively. As some of the inputs to the BF differ between integrations (SNG, coke injections), the blast furnace volumes are also slightly different (426.2 kg/t_{HM} for Case 1 vs. 452 kg/t_{HM} for Case 2). KPI 5 is only associated with case 2. According to the solid yield ratio of the biomass utilized (Table 3), 532 kg/t_{HM} of biomass has to be treated to obtain the required amount of charcoal.

To properly clarify KPIs 6 and 7, Sankey diagrams for both cases are presented in Fig. 6. They represent the carbon flows between the different elements of the steelmaking plant. To establish a common ground for comparison between different streams, the carbon flow is measured in kg_{CO2}/t_{HM}, considering that the carbon present in every stream is eventually transformed to CO_2, following Eq. (8)

$$\text{Carbon flow}\left[\frac{kg_{CO2}}{t_{HM}}\right] = \left(\sum_{i=CO_2,CO,CH_4} n_{,i} + \sum_{i=C_2H_4,C_2H_6} 2n_{,i} + n_C\right) M_{CO2} \tag{8}$$

The different nature of the streams is represented with a colour code indicated in the figure. Grey colours represent solids. Coal, coke and dissolved carbon in the hot metal are ordered from darker to lighter grey, respectively. BFG, COG and BOFG are represented with blue, yellow, and light green, respectively. The BFG fraction that goes to the carbon capture stage in case 1 is represented in maroon and the captured CO_2 from that stream is painted orange. The CH_4 stream leaving the methanation is violet. CO_2 emissions to the atmosphere are presented in red. External fuel is blue, and the solid streams of make-up and purge are displayed in pink. To end, CO_2 equivalent emissions abated by pyrolysis are shown in dark green colour.

The Sankey diagrams illustrate the main difference between cases: the nature of the carbon loop. In Case 1, carbon is mainly recycled by methanation. Part of the carbon contained in the BFG is captured by the CaL system, reconverted to methane and spent again, closing the loop. Meanwhile, in Case 2 carbon is naturally recycled by the growth of biomass ("Regeneration" step in Fig. 6). The loop helps to illustrate the difference between net and gross CO_2 emissions. Even though gross CO_2 emissions (KPI 6) are higher (1971 kg/t_{HM}) in case 2, a great part of those correspond to the carbon introduced by the biomass. That is represented by the dark green loop, which stands for the natural regeneration of the biomass. Those emissions had previously been captured from the atmosphere by the biosphere. When new, sustainable biomass is pyrolyzed and used for the process, the loop closes. Thus, those emissions are considered carbon neutral. The only emissions associated to the pyrolysis process are associated with secondary elements. Taking all into account, net emissions (KPI 7) are lower in Case 2. Compared to Case 0 (1943 kg/t_{HM}), the biomass integration obtains a reduction of 805.4 kg/t_{HM}, which is a 17 % higher reduction than Case 1.

The energy of the sold steel gases (KPI 8) is higher in Case 2 (5322 vs 4684 MJ/t_{HM}). On the one hand, the integration of the carbonator and methanator heat in the power plant in Case 1 allows for a complete substitution of the steel gases, so they do not have to be burned and a greater part of them can be sold. On the other hand, the surplus COG is utilized to feed the CaL, outweighing the positive effect. In both cases, the excess steel gases are much more than in Case 0 (2400 kg/t_{HM}), approximately duplicating in both cases, and are in accord with results from [21], which obtained around 4500–5500 MJ/t_{HM}. The off-gases composition is presented in Table 9. Regarding BFG, their compositions are fairly similar, but present some differences. Namely, Case 1 presents a higher hydrogen share due to the higher SNG injection, while Case 2 presents a higher CO share due to the biochar injection. Conversely, the COG and BOFG compositions of both cases are equal, as the coke oven and the BOF are not affected by the integrations. Regarding recirculations, out of 1287.8 kg/t_{HM} of BFG leaving the BF, 205 kg/t_{HM} (a 16 % of the total) are reinjected for TGR in Case 1, and 793 kg/t_{HM} (61.6 %) of BFG is redirected to the CaL plant. Afterwards, its CO_2 is captured, and the CO_2-free BFG is recycled (586.9 kg/t_{HM}). Regarding Case 2, out of 1538.7 kg/t_{HM}, 270.7 kg/t_{HM} (18 % of the total) of BFG are reinjected for TGR.

Electricity consumption is driven mainly by the electrolyzer, and secondly by the ASU. Case 2 features a 3 times smaller electrolyzer (KPI 9) than Case 1. As it was mentioned when explaining KPI 2, the methanation needs in the biomass integration are much smaller, which directly results in a lower flow of H_2 entering the methanizer. Moreover, the syngas stream includes H_2 (which is therefore not produced in the electrolyzer) and CH_4 (which does not have to be synthetically produced using more H_2). The use of an ASU depends on the oxygen needs of the integration (KPI 11). Not enough O_2 is by-produced in Case 2 to sustain the O_2 needs of the steelmaking plant (mainly, injections to the BOF and to the BF). As a result, the ASU operates to fulfil the O_2 demand. This is the only aspect in which Case 1 is superior to Case 2, operating without oxygen default and not requiring an ASU. Although ASUs are already installed in the steelmaking plants, extra electricity has to be consumed to provide the extra O_2. Nevertheless, ASU electricity consumption is still 10 times lower than the electrolyzer consumption in Case 2, not having a significant effect on the net electricity consumption (KPI 10), which is clearly lower in Case 2.

As it was mentioned in the previous paragraphs, the energy consumption of Case 2 is much lower than Case 1, which, combined with a reduction in CO_2 emissions (1138 vs. 1272 kg_{CO2}/t_{HM}) clearly reflects in the energy penalty (KPI 12), 6.18 MJ/kg_{CO2}, 3.1 times smaller than Case 1. This energy consumption decrease is caused by: i) the pyrolysis plant requires less energy than the CaL plant; ii) coal and coke consumption in the BF is lower in Case 2, thanks to the charcoal injection; iii) SNG

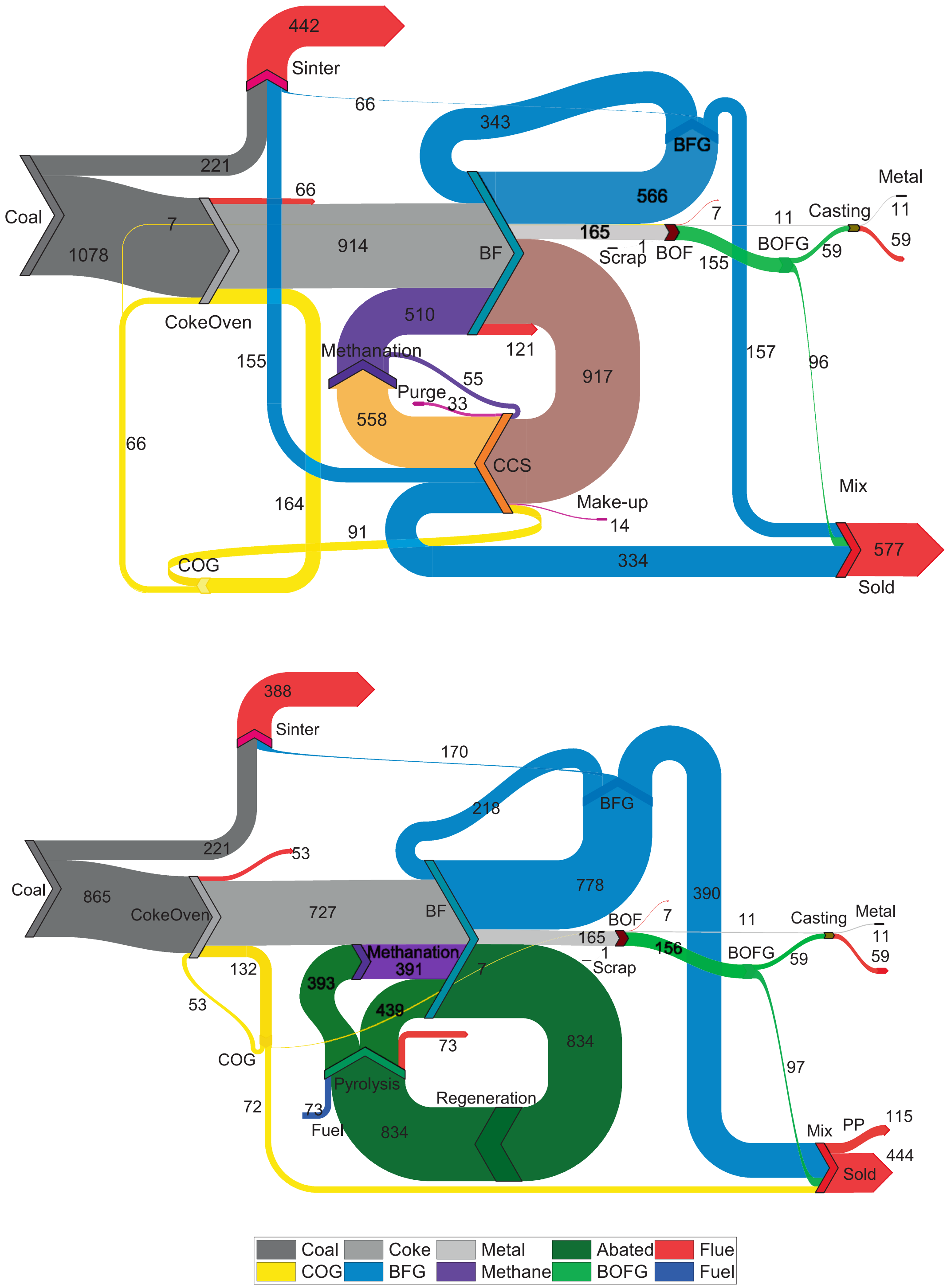

Fig. 6. Sankey diagrams of equivalent CO_2 emissions in kg_{CO2}/t_{HM} (Up: CaL; down: Biomass).

Table 9
Off-gases molar composition.

	BFG Case 1	Case 2	COG Cases 1–2	BOFG Cases 1–2
CO_2 (%)	29.0	28.2	2.3	19.9
CO (%)	27.0	34.9	9.4	66.0
H_2 (%)	22.6	14.7	57.3	2.0
N_2 (%)	1.3	0.3	2.2	8.0
H_2O (%)	20.0	22.0	–	–
CH_4 (%)	–	–	28.7	–
O_2 (%)	–	–	–	4.0

consumption is much lower in Case 2, as Case 1 not only utilizes more SNG in the BF, but also requires additional SNG for the CaL; iv) this results in a smaller electrolyzer, which is further boosted by the syngas composition, which already contains H_2 and CH_4.

As a conclusion, Case 2 scores better in almost every technical result. Results by Perpiñán et al. [21], which modelled an homologous PtG integration to Case 1, but based on amine scrubbing instead of CaL, stated an energy penalty of 17–19 MJ/t_{HM}, similar to Case 1. According to that, this conclusion may be extended to other carbon capture systems, such as amine scrubbing, and the big difference is a result not of a change in the chosen carbon capture technology, but in the concept behind the integration (biomass vs. CC).

4.2. Economic analysis

A breakdown of the CAPEX, OPEX and incomes of each case is presented in Table 10. Both cases are affected by a specific capital expenditure, only associated to each case. In Case 1, a CaL plant is constructed, whereas in Case 2 it is necessary to integrate the biomass treatment plant within the steelmaking plant. Their costs are relatively comparable, and are not the reason for the CAPEX difference. The main difference is associated with the cost of the electrolyzer, which is much bigger in Case 1 (553 M€ vs. 182 M€).

The threefold higher cost in electricity is responsible to the much worse yearly benefits (KPI 14) in Case 1, as it contributes the most to the OPEX of the integration (KPI 16). This is especially true in Case 1, in which electricity is responsible of the 89 % of the OPEX. Costs are more evenly distributed in Case 2 (Fig. 7), in which electricity is responsible of 60 % of the OPEX, while biomass associated costs (transport, treatment, etc.) represent 28 %.

Incomes (KPI 15) are mostly similar in both cases, favouring Case 2. Case 2 is favoured from higher incomes related to the higher amount of CO_2 abated as well as with smaller coal consumption. The difference in the income associated with the sold gases or oxygen is comparatively small. The CO_2 avoidance cost (KPI 17) and the specific implementation cost (KPI 18) are 64.5 €/t_{CO2} and 51.9 €/t_{HM} for Case 2, 4.4 and 3.6 times lower than in Case 1.

According to these results, it is concluded that Case 2 is the best option among the analysed concepts in the literature. Nonetheless, neither of the integrations are profitable with the current economic scenario. To further establish the conditions under which viable scenarios would occur, further sensitivity analyses are performed. Firstly, the main variables responsible for the cost are identified. As it can be identified in Table 10, the five main items are, for the OPEX, the electricity and the biomass cost and, for the incomes, the CO_2 tax, the coal price, and the gases sell price. The weight of the CAPEX is comparatively lower to OPEX and incomes. The influence of the five selected parameters is assessed in Fig. 8, which shows the effect that a ± 50 % variation of them (while keeping constant the other ones) involves in the final C.A.C and S.I.C cost of Case 2. Similar results are expected for Case 1. From this analysis, it is concluded that the most critical variables are the CO_2 tax and the electricity prices.

Subsequently, a sensitivity analysis with respect to CO_2 tax prices and electricity prices with regard to the payback time of the integration is assessed (Fig. 9). As the time window considered for the economic analysis is 20 years, no payback times longer than that are considered. A range of 0 to 100 €/MWh for electricity prices is considered, containing the current standard price for industrial electricity consumption. Similarly, the CO_2 tax range is set from 0 to 600 €/t_{CO2}, covering scenarios without any tax, the current price tax, and a maximum limit of 600 €/t_{CO2}. Strefler et al. [67] suggest that CO_2 tax prices will rise in the following years, reaching 128 €/t_{CO2} by 2050 and between 384 and 907 €/t_{CO2} by 2100. Attending at the current CO_2 tax (84 €/t_{CO2}, [65]) and at the constant development of renewable energies, mid-term profitability would be a plausible scenario.

For Case 1, in order to achieve a positive return of investment in 20 years a minimum tax of 98 €/t_{CO2} is necessary, if electricity were completely subsidized. Considering the current electricity price assumed in this analysis (60.3 €/MWh, point A), the required CO_2 tax is 499 €/t_{CO2}. Assuming renewable electricity obtained from solar photovoltaic production (51 €/MWh, point B) and wind energy (35 €/MWh, point C) [68], 437 €/t_{CO2} or 330 €/t_{CO2} are required to be profitable, respectively.

A scenario of a CO_2 tax of 59 €/t_{CO2} is profitable in Case 2 assuming subsidized energy. When electricity is obtained at the current price (point D), a CO_2 tax of 179 €/t_{CO2} is necessary to achieve profitability. Considering solar photovoltaic (point E) or wind farm production (point F), 161 €/t_{CO2} or 129 €/t_{CO2} are required. It has to be noted that the CO_2

Table 10
Breakdown of CAPEX, OPEX and incomes of each case.

	Case 1	Case 2
CAPEX	**2722 M€**	**1515 M€**
BF Oxy-Retroffiting	125 M€	125 M€
Pyrolysis plant	–	91 M€
Calcium Looping	47 M€	–
Electrolysis	553 M€	182 M€
Methanation	64 M€	43 M€
Other direct costs	1079 M€	600 M€
Indirect costs	849 M€	473 M€
OPEX	**774.67 M€/y**	**410.79 M€/y**
Biomass treatment	–	116.46 M€/y
Limestone renovation	0.67 M€/y	–
Catalyst renovation	0.72 M€/y	0.38 M€/y
Electricity	688.06 M€/y	247.31 M€/y
Water	3.55 M€/y	1.16 M€/y
O&M	81.66 M€/y	45.45 M€/y
INCOMES	**263.80 M€/y**	**326.7 M€/y**
Oxygen	3.06 M€/y	0 M€/y
Sold gases	31.83 M€/y	40.73 M€/y
Coal avoided	84.63 M€/y	112.75 M€/y
CO_2 taxes	144.27 M€/y	173.19 M€/y

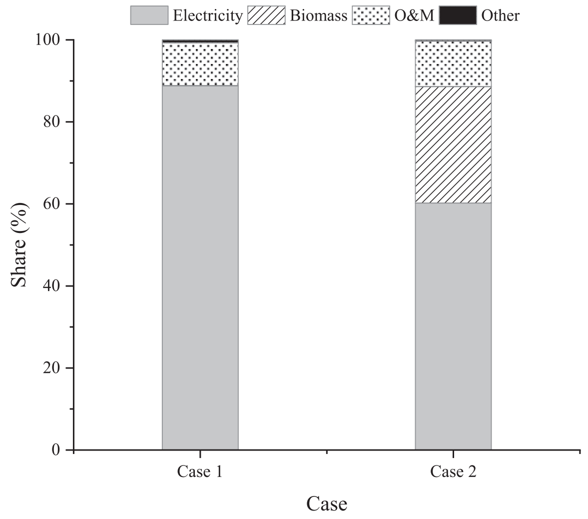

Fig. 7. OPEX distribution.

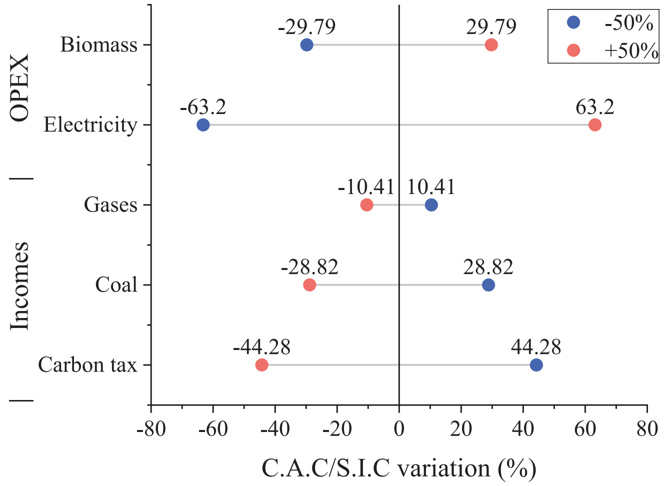

Fig. 8. Sensitivity analysis on the effect of different economic assumptions (for Case 2).

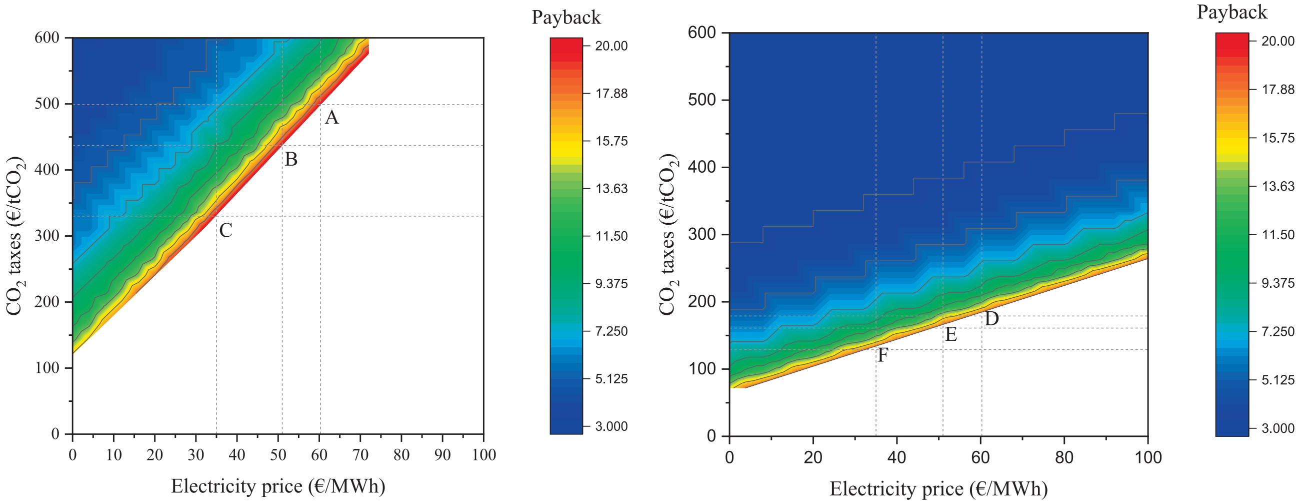

Fig. 9. Sensitivity analysis of payback varying CO_2 tax prices and electricity prices (Left: CaL. Right: Biomass).

tax has risen from 24.5 €/t_{CO2} in 2019 to 83 €/t_{CO2} in 2023, even reaching in March 2023 a price of 105 €/t_{CO2} [69]. Therefore, these values are not far from reality.

It is now clear that the possibility of profitability for the biomass case is not far-fetched. In order to delve into this possibility, a second sensitivity analysis is performed, in which the plant size is varied from 100 t_{HM}/h to 600 t_{HM}/h. The effect on the carbon abatement cost is presented in Fig. 10. An asymptotic decreasing behaviour is obtained as expected due to a cost advantage obtained from scale economy (for a smaller plant, the CAPEX represents a great economic effort, which comparatively diminishes as the size increases). The reader will observe that most of the cost equations utilized here are linear, so the effect of this economy scale is diminished, and is mainly driven by the retrofitting of the furnace, whose cost is considered constant, and the biomass treatment plant, whose cost equation is affected by scale economy. It is expected that, in a real case, the specific costs will reduce as the scale increases, amplifying the scale economy effect. Supposing some of the largest steelmaking plants, able to produce up to 600 t_{HM}/h [70,71], a CO_2 abatement cost of 55 €/t_{CO2} and a specific implementation cost of 45 €/t_{HM} are achievable for the biomass case, taking into account the electricity price and the CO_2 tax of the current economic scenario (60.3 €/MWh and 84 €/t_{CO2}). According to the current steel price (722 €/t_{steel} [72]) and that in this model 1.078 tonnes of steel are obtained per tonne of hot metal, it would imply an overcharge of a 7 % in the steel price. If an infinitely large plant existed, costs would dwindle to 39 €/t_{CO2} and 31 €/t_{HM}. As a final commentary, the option of increasing the power plant size to valorise the excess steel gases was investigated. Even though the electricity cost diminished, the increase in CAPEX (and its respective O&M cost) associated to the power plant expansion, together with the disappearance of the income from sold steel gases, outweighed the benefits, preventing the improvement of the economic results..

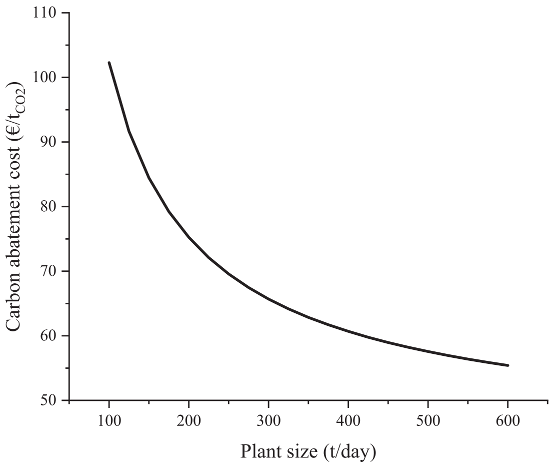

Fig. 10. Sensitivity analysis of carbon abatement cost varying the ironmaking plant size for the biomass case.

4.3. Logistic and environmental challenges, and research potential

As it was presented, both technical and economic results support the biomass integration. Nonetheless, there are different additional elements regarding the use of biomass that must be delved into, in order not to be overly optimistic and simplistic.

In this article, the biomass has been considered as carbon neutral. Raghu et al. [73] addressed the CO_2 emissions of the biomass supply chain for a power plant in Finland and found out that these emissions are between 2.72 and 3.46 kg_{CO2eq} per MWh of biomass, depending on the type of biomass. Taking the highest value, assuming a LHV of 16.4 MJ/$kg_{biomass}$, and a biomass consumption of 532 kg/t_{HM} (as in Case 2), the emissions of this integration related to the biomass supply chain are 8.4 kg_{CO2}/t_{HM}. This is a really low figure compared to the 1138 kg_{CO2}/tHM emissions of the steel plant, so the CO_2 neutrality assumption can be considered as valid. However, this assumption relies on the use of proximity biomass. If biomass must be imported from afar, it would not be longer carbon neutral.

Considering the production rate of 320 t_{HM}/h and 8000 h of annual operation, 1280 Mt of biomass are required yearly. Such large quantities of biomass are not universally available, so this is a local solution for BF mills close to sufficient biomass resources. Mandova et al. [74] addressed this issue, evaluating the status of the top 40 steel production countries via the BF route, and the co-location of sustainably domestically sourced biomass, along with other factors such as national policies supporting alternative fuels. Their results show that a biomass-based BF-BOF steelmaking industry may be a suitable option for countries such as Canada, Sweden, China, USA and France. In contrast, other countries such as Kazakhstan or Brazil must overcome some policy limitations, while others like Mexico or Ukraine lack sufficient biomass resource.

Regarding future research, the authors want to highlight that these results correspond to these CCU integrations, where the CaL capture plant is sized accordingly. A different integration scheme may render different results. As an example, the option of, instead of selling them, using the excess off-gases to fuel a maximized Calcium Looping plant may be interesting in a CCUS scheme. The hybridization of both technologies also presents research potential in a BECCS framework, which may lead to additionally emission reductions. Additionally, the CaL plant may provide thermal energy to the pyrolysis process.

5. Conclusions

In this paper, two low-carbon concepts integrated in the blast furnace steelmaking route were assessed and compared from a technical and economic point of view. These new concepts incorporate power-to-gas technology, top gas recycling and oxygen blast furnace (oxy-BF) and are compared against a conventional steelmaking plant, in which no decarbonisation technologies have been included.

The first low carbon proposal included a carbon capture stage via Calcium Looping. The captured CO_2 was used as the carbon source for the methanation plant that produces the synthetic natural gas to be injected as reducing agent in the blast furnace. The Calcium Looping plant includes kinetics for calcination and carbonation. The second concept is based on biomass pyrolysis. Charcoal and syngas are produced from the pyrolysis. The former is pulverized and injected into the blast furnace, replacing part of the coke. The latter is used as the carbon source for the methanation stage, thus getting rid of the carbon capture stage.

Both cases present relevant advances compared to the reference plant, with reductions in coke and carbon consumption, and CO_2 emissions. When compared, the biomass integration scores better in almost every technical and economic result. Coke consumption is lower in the second proposed concept as part of the coke is replaced by the charcoal. Therefore, coal consumption is further reduced (295 kg/t_{HM} are avoided compared to Case 0, a 33 % more than in Case 1). Net CO_2 emissions are also lower thanks to the carbon–neutral nature of the biomass, obtaining reductions of up to 805 kg_{CO2}/t_{HM}. Due to all of the reasons mentioned before, energy penalty is reduced to 6.19 MJ/kg_{CO2}, 3.1 times less compared to the CaL case.

Furthermore, the electrolyzer size is also reduced 3 times, therefore reducing proportionally the electricity consumption. The significant reduction in electricity consumption is due to two main reasons: (i) less SNG has to be produced and (ii) part of the required H_2 is provided by the syngas. According to that, this conclusion may be extended to other carbon capture systems, such as amine scrubbing, which presents similar technical results as the CaL integration, like the energy penalty.

The better technical results lead to better economic results, reducing the OPEX (mainly driven by electricity consumption), and increasing the incomes (mainly driven by the higher CO_2 emissions avoided). CAPEX is also halved, mainly due to the smaller electrolyzer (the cost of the capture plant is comparable to the cost of the biomass treatment plant). As a result, the CO_2 avoidance cost and the specific implementation costs are reduced 4.9 and 3.4 times, respectively, in the biomass case with respect to the CaL case. Considering some of the largest steelmaking plants, which produce up to 600 t_{HM}/h, a CO_2 abatement cost of 55 €/t_{CO2} and a specific implementation cost of 45 €/t_{HM} is achievable.

Still, no integration is profitable with the current scenario. If electricity is purchased at 60.3 €/MWh, then a CO_2 tax of 499 €/t_{CO2} would be required for the CaL plant to obtain long-term profitability. Regarding the biomass plant, a CO_2 tax of 179 €/t_{CO2} would be needed, and if electricity was obtained from solar (51 €/MWh) or wind (35 €/MWh) energy, 169 €/t_{CO2} or 129 €/t_{CO2} are required. Attending at the current CO_2 tax (84 €/t_{CO2}) which will probably rise in the future, and at the constant development of renewable energies, which will probably drive the electricity price down, it is plausible for the biomass plant to be profitable in the mid-term.

In summary, the biomass approach, involving pyrolysis and syngas production, presents promising results. It demonstrates reduced energy requirements, lower CO_2 emissions, and improved economic feasibility, leading to decreased operational and capital expenses, in comparison with the CaL integration. Despite current economic challenges, the potential for profitability in the mid-term, driven by the ongoing development of renewable energy, positions the biomass integration as a promising solution for environmentally conscious steelmaking. Nonetheless, it cannot be forgotten that the main issue with biomass is its availability: it is seasonal and scarce, widely distributed (leading to logistical challenges and increased costs), and only certain types are suitable for operation. Therefore, this integration is not suitable for every place, and it should be encouraged in regions which are rich in biomass and provide good national policies supporting alternative fuels, such as Canada, Sweden, China, USA or France. The authors suggest the hybridization of both technologies to overcome some of these limitations as a potential line of research. These hybridizations may present additional benefits, such as higher emission abatement potential or better energetic efficiency of the plant.

CRediT authorship contribution statement

Cristian Barón: Writing – original draft, Visualization, Validation, Software, Methodology, Formal analysis, Conceptualization. **Manuel Bailera:** Writing – review & editing, Writing – original draft, Software, Methodology, Funding acquisition, Conceptualization. **Jorge Perpiñán:** Software, Methodology. **Begoña Peña:** Writing – review & editing, Writing – original draft, Supervision, Methodology, Funding acquisition, Formal analysis, Conceptualization.

Declaration of competing interest

The authors declare that they have no known competing financial interests or personal relationships that could have appeared to influence the work reported in this paper.

Acknowledgments

This publication is supported by RYC2022-038283-I, funded by MCIN/AEI/ 10.13039/ 501100011033 and the European Social Fund Plus (ESF+), and by Government of Aragon (Research Group DGA T46_17R). This work is also part of the R&D project TED2021-130000B-I00, funded by MCIN/AEI 10.13039/501100011033/ and by the “European Union NextGenerationEU/PRTR”. The Investigo Program funding by the “European Union NextGenerationEU/PRTR” and the FPU Programme of the Spanish Ministry of Science, Innovation and Universities (FPU/00073) provided financial support for C.B. Ph.D studies.

Appendix A. Supplementary data

Supplementary data to this article can be found online at https://doi.org/10.1016/j.fuel.2025.137810.

Data availability

Supplementary material is included

References

[1] IEA. Iron and Steel Technology Roadmap 2020.

[2] Perpiñán J, Peña B, Bailera M, Eveloy V, Kannan P, Raj A, et al. Integration of carbon capture technologies in blast furnace based steel making: a comprehensive and systematic review. Fuel 2023;336:127074. https://doi.org/10.1016/j.fuel.2022.127074.

[3] Guevara Opinska L, Mahmoud M, Bene C, Rademaekers K. Moving towards Zero-Emission Steel 2021.

[4] Scheele. Decarbonization of ironmaking, in MM Steel Club, (2021). Director of global commercialization, Linde.

[5] Santos MPS, Hanak DP. Carbon capture for decarbonisation of energy-intensive industries: a comparative review of techno-economic feasibility of solid looping cycles. Front Chem Sci Eng 2022;16:1291–317. https://doi.org/10.1007/s11705-022-2151-5.

[6] Pascual S, Romeo LM, Lisbona P. Optimized Ca-looping thermochemical energy storage under dynamic operation for concentrated solar power. J Energy Storage 2023;68:107587. https://doi.org/10.1016/j.est.2023.107587.

[7] Tian S, Jiang J, Yan F, Li K, Chen X, Manovic V. Highly efficient CO_2 capture with simultaneous iron and CaO recycling for the iron and steel industry. Green Chem 2016;18:4022–31. https://doi.org/10.1039/c6gc00400h.

[8] Sánchez-Biezma A, Paniagua J, Diaz L, Lorenzo M, Alvarez J, Martínez D, et al. Testing postcombustion CO_2 capture with CaO in a 1.7 MW_t pilot facility. In: Energy Procedia. Elsevier Ltd; 2013. p. 1–8. https://doi.org/10.1016/j.egypro.2013.05.078.

[9] Ströhle J, Junk M, Kremer J, Galloy A, Epple B. Carbonate looping experiments in a 1 MW_{th} pilot plant and model validation. Fuel 2014;127:13–22. https://doi.org/10.1016/j.fuel.2013.12.043.

[10] Dieter H, Bidwe AR, Varela-Duelli G, Charitos A, Hawthorne C, Scheffknecht G. Development of the calcium looping CO_2 capture technology from lab to pilot scale at IFK, University of Stuttgart. Fuel 2014;127:23–37. https://doi.org/10.1016/j.fuel.2014.01.063.

[11] Wang W, Ramkumar S, Li S, Wong D, Iyer M, Sakadjian BB, et al. Subpilot demonstration of the carbonation-calcination reaction (CCR) process: High-temperature CO_2 and sulfur capture from coal-fired power plants. Ind Eng Chem Res 2010;49:5094–101. https://doi.org/10.1021/ie901509k.

[12] Symonds RT, Lu DY, Hughes RW, Anthony EJ, Macchi A. CO_2 capture from simulated syngas via cyclic carbonation/calcination for a naturally occurring limestone: Pilot-plant testing. Ind Eng Chem Res 2009;48:8431–40. https://doi.org/10.1021/ie900645x.

[13] Chang MH, Huang CM, Liu WH, Chen WC, Cheng JY, Chen W, et al. Design and experimental investigation of calcium Looping process for 3-kW_{th} and 1.9-MW_{th} facilities. Chem Eng Technol 2013;36:1525–32. https://doi.org/10.1002/ceat.201300081.

[14] Calby2030. https://cordis.europa.eu/project/id/101075416.

[15] Sungsook C, Srinophakun TR. Study of lime flow rate on calcium looping carbon capture for steel plant, Ironmaking & Steelmaking: Processes. Products and Applications 2024. https://doi.org/10.1177/03019233241251598.

[16] Carbone C, Ferrario D, Lanzini A, Verda V, Agostini A, Stendardo S. Calcium looping in the steel industry: GHG emissions and energy demand. Int J Greenhouse Gas Control 2023;125:103893. https://doi.org/10.1016/j.ijggc.2023.103893.

[17] Henriques MF, Dantas F, Schaeffer R. Potential for reduction of CO_2 emissions and a low-carbon scenario for the Brazilian industrial sector. Energy Policy 2010;38:1946–61. https://doi.org/10.1016/j.enpol.2009.11.076.

[18] Gonçalves J, Da M, Machado S, Osório E, Cezar A, Vilela F. Reactivity of Brazilian coal, Charcoal, Imported Coal and Blends Aiming to their Injection into Blast Furnaces. Mater Res 2010;13:287–92.

[19] Liu Y, Shen Y. Modelling and optimisation of biomass injection in ironmaking blast furnaces. Prog Energy Combust Sci 2021;87:100952. https://doi.org/10.1016/j.pecs.2021.100952.

[20] Bailera M, Rebolledo B. Integration of power to gas and biomass charcoal in oxygen blast furnace ironmaking. Energy Convers Manag 2024;300:117916. https://doi.org/10.1016/j.enconman.2023.117916.

[21] Perpiñán J, Bailera M, Peña B, Romeo LM, Eveloy V. High oxygen and SNG injection in blast furnace ironmaking with Power to Gas integration and CO_2 recycling. J Clean Prod 2023;405:137001. https://doi.org/10.1016/j.jclepro.2023.137001.

[22] Takahashi K, Nouchi T, Sato M, Ariyama T. Perspective on progressive development of oxygen blast furnace for energy saving. ISIJ Int 2015;55:1866–75. https://doi.org/10.2355/isijinternational.ISIJINT-2015-196.

[23] Quader MA, Ahmed S, Raja Ghazilla RA, Ahmed S, Dahari M. Evaluation of criteria for CO_2 capture and storage in the iron and steel industry using the 2-tuple DEMATEL technique. J Clean Prod 120 2016:207–20. https://doi.org/10.1016/j.jclepro.2015.10.056.

[24] Sato M, Takahashi K, Nouchi T, Ariyama T. Predictcion of next-generation ironmaking process based on oxygen blast furnace suitable for CO_2 mitigation and energy flexibility. ISIJ Int 2015;55:2105–14. https://doi.org/10.2355/isijinternational.ISIJINT-2015-264.

[25] Bailera M, Nakagaki T, Kataoka R. Revisiting the Rist diagram for predicting operating conditions in blast furnaces with multiple injections. Open Res Europe 2021. https://doi.org/10.12688/openreseurope.14275.1.

[26] Bailera M, Nakagaki T, Kataoka R. Extending the Operating Line Methodology to consider Shaft and Preheating Injections in Blast Furnaces. ISIJ Int 2022;62:2454–65. https://doi.org/10.2355/isijinternational.ISIJINT-2022-111.

[27] Perpiñán J, Bailera M, Peña B, Romeo LM, Eveloy V. Technical and economic assessment of iron and steelmaking decarbonisation via power to gas and amine scrubbing. Energy 2023;276:127616. https://doi.org/10.1016/j.energy.2023.127616.

[28] Wu J, Wang R, Pu G, Qi H. Integrated assessment of exergy, energy and carbon dioxide emissions in an iron and steel industrial network. Appl Energy 2016;183:430–44. https://doi.org/10.1016/j.apenergy.2016.08.192.

[29] LEECO Steel. https://www.leecosteel.com/news/post/carbon-steel-categories/ (Accessed Apr 2024).

[30] https://nelhydrogen.com/ (accessed Mar. 02, 2022).

[31] Izumiya K, Shimada I, Methane producing technology from CO_2 for carbon recycling 2021:34–5., in: The First Symposium on Carbon Ultimate Utilization Technologies for the Global Environment, CUUTE-1, 2021: pp. 34–35.

[32] LTD 2022. Accessed Sep 2022, http://www.cisdigroup.com/4-steelmaking.html.

[33] Haran S, Rao AB, Banerjee R. Techno-economic analysis of a 660 MWe supercritical coal power plant in India retrofitted with calcium looping (CaL) based CO_2 capture system. Int J Greenhouse Gas Control 2021;112. https://doi.org/10.1016/j.ijggc.2021.103522.

[34] C. Barón, M. Bailera, J. Perpiñán, P. Lisbona, B. Peña, Modelling of carbon capture through Calcium Looping technology for the integration of Power to Gas in a blast furnace-based iron and steel industry, Under Revision.

[35] Ortiz C, Valverde JM, Chacartegui R, Benítez-Guerrero M, Perejón A, Romeo LM. The oxy-CaL process: a novel CO_2 capture system by integrating partial oxy-combustion with the calcium-looping process. Appl Energy 2017;196:1–17. https://doi.org/10.1016/j.apenergy.2017.03.120.

[36] Kremer J, Galloy A, Ströhle J, Epple B. Continuous CO_2 capture in a 1-MW_{th} carbonate looping pilot plant. Chem Eng Technol 2013;36:1518–24. https://doi.org/10.1002/ceat.201300084.

[37] Junk M, Kremer J, Ströhle J, Eimer N, Priesmeier U, Weingärtner C, et al. Design of a 20 MW_{th} carbonate looping pilot plant for CO_2-capture of coal fired power plants by means of limestone, in. Energy Procedia, Elsevier Ltd 2014:2178–89. https://doi.org/10.1016/j.egypro.2014.11.237.

[38] Abanades JC. The maximum capture efficiency of CO_2 using a carbonation/calcination cycle of CaO/$CaCO_3$. Chem Eng J 2002;90:303–6.

[39] Reitza M, Junka M, Ströhlea J, Epplea B. Design and erection of a 300 kW_{th} indirectly heated carbonate looping test facility, in. Energy Procedia, Elsevier Ltd 2014:2170–7. https://doi.org/10.1016/j.egypro.2014.11.236.

[40] Junk M, Reitz M, Ströhle J, Epple B. Thermodynamic evaluation and cold flow model testing of an indirectly heated carbonate looping process. Chem Eng Technol 2013;36:1479–87. https://doi.org/10.1002/ceat.201300019.

[41] Žalec D, Hanak DP, Može M, Golobič I. Process development and performance assessment of flexible calcium looping biomass gasification for production of renewable gas with adjustable composition. Int J Energy Res 2022;46:6197–215. https://doi.org/10.1002/er.7558.

[42] Hanak DP, Michalski S, Manovic V. Supercritical CO_2 cycle for coal-fired power plant based on calcium looping combustion. Therm Sci Eng Prog 2020;20:100723. https://doi.org/10.1016/j.tsep.2020.100723.

[43] Atsonios K, Zeneli M, Nikolopoulos A, Nikolopoulos N, Grammelis P, Kakaras E. Calcium looping process simulation based on an advanced thermodynamic model combined with CFD analysis. Fuel 2015;153:370–81. https://doi.org/10.1016/j.fuel.2015.03.014.

[44] Yan L, Cao Y, He B, Li X. Calcium Looping Enhanced Biomass Steam Gasification in a Two-Stage Fluidized Bed Gasifier. Energy Fuels 2018;32:8462–73. https://doi.org/10.1021/acs.energyfuels.8b01414.

[45] Smolders K, Baeyens J. Overall solids movement and solids residence time distribution in a CFB-riser. Chem Eng Sci 2000;55:4101–16.

[46] Myöhänen K. Modelling of combustion and sorbent reactions in three-dimensional flow environment of a circulating fluidized bed furnace. Lappeenranta 2011.

[47] Solar J, Caballero BM, López-Urionabarrenechea A, Acha E, Arias PL. Pyrolysis of Forestry Waste in a Screw Reactor with four Sequential heating zones: Influence of Isothermal and Nonisothermal Profiles. Ind Eng Chem Res 2021;60:18627–39. https://doi.org/10.1021/acs.iecr.1c01932.

[48] Busca G, Spennati E, Borella M, Casazza AA, Garbarino G. On the Exploitation of Lignin Slow Pyrolysis Products. Energies (Basel) 2025;18:943. https://doi.org/10.3390/en18040943.

[49] Yang Q, Han F, Chen Y, Yang H, Chen H. Greenhouse gas emissions of a biomass-based pyrolysis plant in China. Renew Sustain Energy Rev 2016;53:1580–90. https://doi.org/10.1016/j.rser.2015.09.049.

[50] Crombie K, Mašek O. Investigating the potential for a self-sustaining slow pyrolysis system under varying operating conditions. Bioresour Technol 2014;162:148–56. https://doi.org/10.1016/j.biortech.2014.03.134.

[51] Salimbeni A, Lombardi G, Rizzo AM, Chiaramonti D. Techno-Economic feasibility of integrating biomass slow pyrolysis in an EAF steelmaking site: a case study. Appl Energy 2023;339:120991. https://doi.org/10.1016/j.apenergy.2023.120991.

[52] De Lena E, Spinelli M, Gatti M, Scaccabarozzi R, Campanari S, Consonni S, et al. Techno-economic analysis of calcium looping processes for low CO_2 emission cement plants. Int J Greenhouse Gas Control 2019;82:244–60. https://doi.org/10.1016/j.ijggc.2019.01.005.

[53] Aspen Energy Analyser. AspenTech.

[54] Proost J. State-of-the art CAPEX data for water electrolysers, and their impact on renewable hydrogen price settings. Int J Hydrogen Energy 2019;44:4406–13. https://doi.org/10.1016/J.IJHYDENE.2018.07.164.

[55] De Saint Jean M, Baurens P, Bouallou C, Couturier K. Economic assessment of a power-to-substitute-natural-gas process including high-temperature steam electrolysis. Int J Hydrogen Energy 2015;40:6487–500. https://doi.org/10.1016/J.IJHYDENE.2015.03.066.

[56] Lehner M, Tichler R, Steinmüller H, Koppe M. Power-to-gas: Technology and Business Models, Springler Briefs, Energy 2014:03995-4. https://doi.org/10.1007/978-3-319-.

[57] Peters M, Timmerhaus K. R. 5th Edition. Plant Design and Economics for Chemical Engineers: West; 2003.

[58] Norgate T, Langberg D. Environmental and Economic Aspects of Charcoal Use in steelmaking. ISIJ Int 2009;49:587–95.

[59] Ortiz C, Valverde JM, Chacartegui R, Perez-Maqueda LA, Giménez P. The calcium-looping ($CaCO_3$/CaO) process for thermochemical energy storage in concentrating solar power plants: a critical review. Renew Sustain Energy Rev 2019;113:109252. https://doi.org/10.1016/j.rser.2019.109252.

[60] Bailera M, Espatolero S, Lisbona P, Romeo LM. Power to gas-electrochemical industry hybrid systems: a case study. Appl Energy 2017;202:435–46. https://doi.org/10.1016/J.APENERGY.2017.05.177.

[61] https://tradingeconomics.com/spain/electricity-price (Accessed Dec 2023).

[62] G. Benjaminsson, J. Benjaminsson, R.B. Rudberg, Power-to-Gas-A technical review (El-till-Gas-System, ekonomi och teknik) SGC Rapport 2013:284 “Catalyzing energygas development for sustainable solutions,”. www.sgc.se.

[63] M. Hurskainen, Industrial oxygen demand in Finland. Research report VTT-R-06563-17. VTT Technical Research Center of Finland Ltd. https://publications.vtt.fi/julkaisut/muut/2017/VTT-R-06563-17.pdf.

[64] U.S. Department of Energy, Quarterly Coal Report July–September 2023. https://www.eia.gov/coal/production/quarterly/pdf/qcr-all.pdf, 2023. www.eia.gov.

[65] https://www.theice.com/products/197/EUA-Futures/data?marketId=7100229 (Accessed Dec 2023).

[66] Geerdes M, Chaigneau R, Lingiardi O, R. van O. Molenaar, W.J. R.S SY,. Modern Blast Furnace Ironmaking an Introduction. IOS Press; 2020.

[67] Strefler J, Kriegler E, Bauer N, Luderer G, Pietzcker RC, Giannousakis A, et al. Alternative carbon price trajectories can avoid excessive carbon removal. Nat Commun 2021;12:2264. https://doi.org/10.1038/s41467-021-22211-2.

[68] IRENA, Renewable Power Generation Costs in 2021., 2022. www.irena.org.

[69] Auctions by the Common Auction Platform, EEX, October, November, December 2023 https://climate.ec.europa.eu/document/download/f3199005-4ca8-461b-9499-e5f3846ea4a5_en?filename=cap_report_202312_en.pdf.

[70] Danieli Corus Ironworks. https://www.danieli.com/en/news-media/news-events/severstal-awards-contract-blast-furnace-no-5-reline-danieli-corus_37_205.htm (Accessed Apr 2024).

[71] Shagang Group Ironworks. https://www.glimpse-technology.com/the-world-s-largest-blast-furnace.html (Accessed Apr 2024).

[72] Steel Prices. https://www.focus-economics.com/commodities/base-metals/steel-europe/ (Accessed May 2024).

[73] Raghu KC, Aalto M, Korpinen OJ, Ranta T, Proskurina S. Lifecycle assessment of biomass supply chain with the assistance of agent-based modelling. Sustainability (Switzerland) 2020;12:1964. https://doi.org/10.3390/su12051964.

[74] Mandova H, Gale WF, Williams A, Heyes AL, Hodgson P, Miah KH. Global assessment of biomass suitability for ironmaking – Opportunities for co-location of sustainable biomass, iron and steel production and supportive policies. Sustainable Energy Technol Assess 2018;27:23–39. https://doi.org/10.1016/j.seta.2018.03.001.